



OPEN ACCESS

EDITED BY

Wenjun Liu,
Beijing University of Posts and
Telecommunications (BUPT), China

REVIEWED BY

Zuxing Zhang,
Nanjing University of Posts and
Telecommunications, China
Xiaohui Li,
Shaanxi Normal University, China

*CORRESPONDENCE

Pengfei Ma,
shandapengfei@126.com
Pu Zhou,
zhoupu203@163.com

SPECIALTY SECTION

This article was submitted to Optics and
Photonics,
a section of the journal
Frontiers in Physics

RECEIVED 10 August 2022

ACCEPTED 29 August 2022

PUBLISHED 16 September 2022

CITATION

Li W, Ren S, Deng Y, Chen Y, Lu Y, Liu W,
Ma P, Pan Z, Chen Z, Lei Si and Zhou P
(2022), Investigation of the confined-
doped fiber on single-mode operating
and power scaling in all-fiber single-
frequency amplifiers.
Front. Phys. 10:1016047.
doi: 10.3389/fphy.2022.1016047

COPYRIGHT

© 2022 Li, Ren, Deng, Chen, Lu, Liu, Ma,
Pan, Chen, Lei Si and Zhou. This is an
open-access article distributed under
the terms of the [Creative Commons
Attribution License \(CC BY\)](https://creativecommons.org/licenses/by/4.0/). The use,
distribution or reproduction in other
forums is permitted, provided the
original author(s) and the copyright
owner(s) are credited and that the
original publication in this journal is
cited, in accordance with accepted
academic practice. No use, distribution
or reproduction is permitted which does
not comply with these terms.

Investigation of the confined-doped fiber on single-mode operating and power scaling in all-fiber single-frequency amplifiers

Wei Li¹, Shuai Ren¹, Yu Deng¹, Yisha Chen¹, Yao Lu¹, Wei Liu^{1,2,3}, Pengfei Ma^{1,2,3*}, Zhiyong Pan^{1,2,3}, Zilun Chen^{1,2,3}, Lei Si^{1,2,3} and Pu Zhou^{1*}

¹College of Advanced Interdisciplinary Studies, National University of Defense Technology, Changsha, China, ²Nanhu Laser Laboratory, National University of Defense Technology, Changsha, China, ³Hunan Provincial Key Laboratory of High Energy Laser Technology, Changsha, China

In this paper, we proposed a strategy for achieving all-fiber single-frequency amplifiers with near-diffraction-limited beam quality by using confined-doped fiber. Benefiting from the large mode area (LMA) and mode selection properties of the confine-doped fiber, the stimulated Brillouin scattering (SBS) and transverse mode instability (TMI) effects were comprehensively suppressed. Based on this confined-doped fiber assisted amplifier, a 322 W SBS-limited single-frequency laser was obtained with M^2 factor of 1.25/1.33 for the x/y direction. Comparing with the full-doped fiber assisted one, the TMI threshold of the confined-doped one is improved more than 1.6 times. Overall, the technique of confined-doped in the fiber core provides a promising approach for the power scaling and single-mode operation of all-fiber single-frequency lasers.

KEYWORDS

confined-doped fiber, single-frequency amplifier, stimulated brillouin scattering, transverse mode instability, single-mode operating

Introduction

High power single-frequency fiber lasers and amplifiers are highly desired in numerous applications, like coherent beam combination [1], gravitation wave detection [2, 3], coherent lidar systems [4], nonlinear frequency conversion [5, 6] and so on. However, the power scaling of the single-frequency fiber lasers is primarily limited by the SBS and TMI effects. Till now, a variety of approaches have been reported to provide effective suppression on these two effects, separately. For example, approaches like enlarging the mode area or shortening fiber length [7–9], employing acoustically tailoring technique [10], introducing strain or temperature gradient [11–13], using gain competition strategy [14–16] and counter-pumping scheme [17, 18] are always applied to suppress the SBS effect. Meanwhile, plenty of effective methods are

utilized in the high-power laser systems to mitigate the TMI effect, such as coiling active fiber [19, 20], optimizing pumping wavelength or signal wavelength [21–23], suppressing the noise property [24, 25], reducing the fiber core to pump cladding ratio [26, 27], and using gain-tailoring technique [28, 29]. Nevertheless, in a traditional step-index active fiber assisted single frequency system, inter-contrary seems to be existed for the simultaneous suppression of TMI and SBS effects [30–32].

By using special designed active fibers to comprehensively suppress the SBS and TMI effects, single-frequency fiber lasers have flourished in the last decade and series of attractive results have been achieved. Based on the space-coupled configuration, C. Robin et al realized an 811 W single-frequency fiber laser through an acoustic and gain-tailored photonic crystal fiber (PCF) with a beam quality of $M^2 < 1.2$ in 2014 [29]. In 2022, T. Matniyaz et al utilizing an all-solid photonic bandgap fiber achieved a 500 W single-frequency laser with beam quality value of ~ 1.6 [33]. Due to the compactness and stability features of the all-fiber configuration, it is a preferable choice for applications. Thus, numerous researches on all-fiber single-frequency lasers have been reported in recent years. For instance, in 2020, W. Lai et al utilizing a LMA tapered active fiber realized a 550 W stochastic polarized single-frequency laser and the M^2 value is measured to be 1.47 [34]. Besides, S. Hochheim et al reported a Chirally-Coupled-Core fiber constructed all-fiber amplifier in 2022 [35], in which a 336 W single-frequency laser with high signal to noise ratio was obtained. All these results proved that the SBS and TMI effects in high-power single-frequency fiber amplifiers could be effectively mitigated by using special designed fibers.

Except for the above-mentioned special designed fibers, confined-doped technique is another promising strategy in fiber design, which is proposed to have advantage in the comprehensive suppression of the SBS and TMI effects. Generally, the confine-doped fibers have a large mode area, which facilitates the suppression of nonlinear effects. Meanwhile, by changing the doping ratio of the fiber core, different gains could be provided to the fundamental mode and high-order modes, which can play a mode selection role and results in an enhancement of the TMI threshold [36]. In the previous researches, confined-doped fibers have been reported to be applied in the high-power fiber laser systems with nanoscale linewidth and performed an impressive suppression on the nonlinear effects and TMI effect [37, 38]. In 2022, the confine-doped fiber was also reported to be utilized in a space-coupled single-frequency amplifier [39] and a 123 W single-frequency laser with M^2 value < 1.11 was realized. Those results illustrate that the confined-doped fiber with optimized fabrication parameters will be promising for achieving high-power all-fiber single-frequency lasers with excellent beam quality.

In this work, we build an all-fiber single-frequency amplifier by using a confine-doped fiber. Based on this amplifier, we investigated the performances of the confined-doped fiber on power scaling and beam quality maintaining. As a result, a 322 W SBS-limited single-frequency laser is achieved with high spectral signal-to-noise ratio (SNR) and near-diffraction-limited beam quality.

Experimental setup

System configuration

The experimental setup of the high-power single-frequency fiber amplifier is built on the master oscillator power amplifier (MOPA) configuration, as shown schematically in Figure 1. The single-frequency source (SFS) is a linearly polarized fiber laser with a central wavelength of 1,064 nm [40]. The output power and the 3 dB linewidth of this seed are measured to be 53 mW and 20 kHz, respectively. Then the seed is injected into a commercial pre-amplifier (Pre-1) and the output power is amplified to ~ 1 W. After Pre-1, an isolator (ISO) is employed to prevent the backward propagating laser and protect the front system. Moreover, a band-pass filter (BPF-1) operating at $1,064 \pm 1$ nm is spliced near behind, which could provide an effective suppression of the amplified spontaneous emission (ASE) in the subsequent system. The signal laser is further amplified to ~ 10 W through the second pre-amplifier (Pre-2). After that, a high-power circulator is inserted to export the backward propagating laser (for power and spectrum measurement). Before the main amplifier, a high-power band-pass filter (BPF-2) with a bandwidth of $1,064 \pm 1$ nm is employed to remove the sideband noise and suppress the ASE in the main amplifier.

The main amplifier is constructed in co-pumping scheme and six 976 nm LDs are combined to pump a Yb-doped fiber (YDF) via a $(6 + 1) \times 1$ pump and signal combiner. In this combiner, the core/inner cladding diameter of the signal input port is $10/130 \mu\text{m}$ while that of the output port is $42/250 \mu\text{m}$. The pump delivery fibers of the LDs and the combiner are all $105/125 \mu\text{m}$ passive fibers with numerical aperture (NA) of 0.22. A piece of 1.5-m-long confined-doped YDF is applied in the main amplifier to provide active gain. Especially, in the process of constructing the main amplifier, the fused points are carefully processed to avoid the excitation of high order modes while the active fiber is properly coiled on a water-cooled plate with a diameter of 15 cm to filter out high order modes. Finally, the amplified laser is output through a quartz block holder (QBH). The collimated output laser is then transmitted to a dichroic mirror to remove the residual pump before all the measurements.

Design of the active fiber

The active fiber used in the main amplifier is a confined-doped fiber with absorption coefficient of ~ 10 dB/m while pump by the LDs with the central wavelength of 976 nm. The cross-section of this confined-doped fiber is demonstrated in Figure 2A. As shown in the picture, the core diameter of the confined-doped fiber is fabricated as large as $42 \mu\text{m}$ while the inner-cladding is fabricated with a diameter (side-to-side) of $250 \mu\text{m}$. Especially, according to the previous studies [41, 42], diverse inner cladding shapes perform differently in coupling efficiencies of the double-cladding fibers. And a small spiral

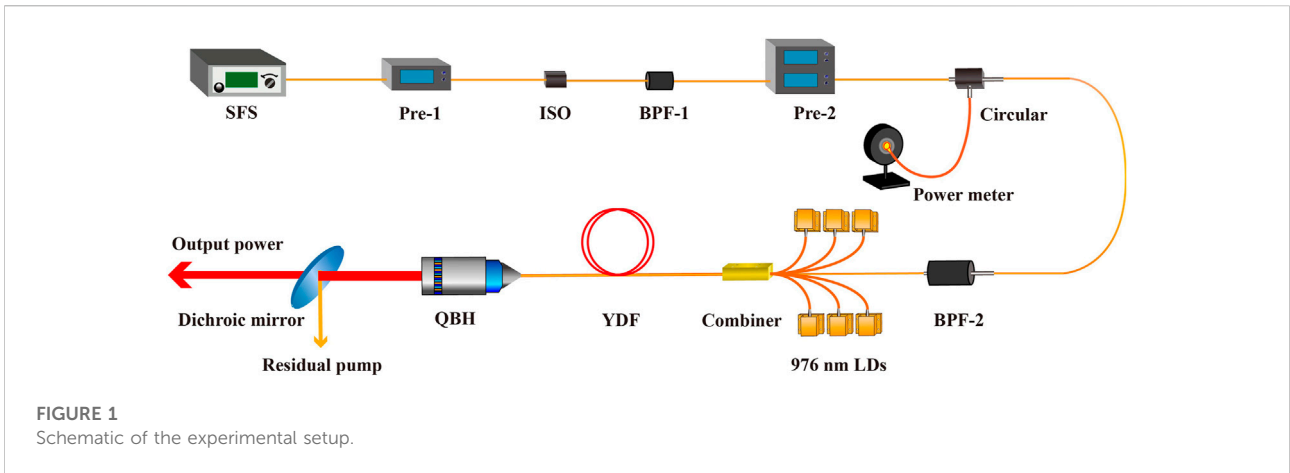


FIGURE 1 Schematic of the experimental setup.

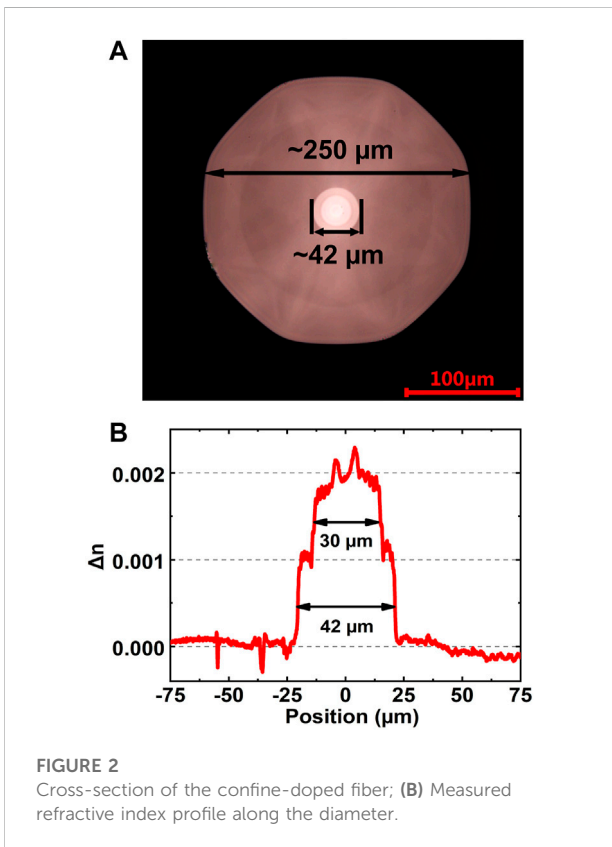


FIGURE 2 Cross-section of the confine-doped fiber; (B) Measured refractive index profile along the diameter.

distortion of an otherwise circular inner cladding shape is shown to enhance the coupling efficiency significantly relative to other geometries. Therefore, the octagon shaped cladding is applied in the fabrication of our confined-doped fiber to enhance the coupling efficiency. Figure 2B illustrates the refractive index profile along the diameter which could be divided into three parts. From the outermost layer to the center, the refractive index increases in a gradient,

representing to the inner-cladding, undoped core and Yb-doped core, respectively. The doped area is measured to be 30 μm, corresponding to a doping ratio of 71.5%. Moreover, the effective mode area (A_{eff}) is defined as:

$$A_{eff} = \frac{\left[\iint E^2(r, \varphi) r dr d\varphi \right]^2}{\iint E^4(r, \varphi) r dr d\varphi} \quad (1)$$

$E(r, \varphi)$ represent to the transverse distribution of the electric field of the fundamental mode. As a result, the A_{eff} is calculated to be 519.5 μm².

Simulation analysis and experiment results

Simulation on the distributions of different modes

According to the measured refractive index profile along the diameter, the modes distributions in the active fibers are simulated under 30 different modes injection. Although all those 30 modes are degenerate with each other, some of them only differ in angles and have the same intensity distribution along the radial direction. Therefore, when analysing the intensity distribution in the radial direction, those modes have only angular differences are ignored. As a result, there are 9 modes remained with different radial intensity distributions, as shown in Figure 3A. The upper half of Figure 3A demonstrates the intensity distribution of different modes in the full-doped fiber, where the black circle indicates the full-doped fiber core (42 μm). The bottom half shows the intensity distribution of different modes in the confined-doped fiber, where the inner black circle indicates the doped region (30 μm) and the outer black circle indicates the undoped region (42 μm). Comparing the beam profiles shown in Figure 3A, we can see that the profiles

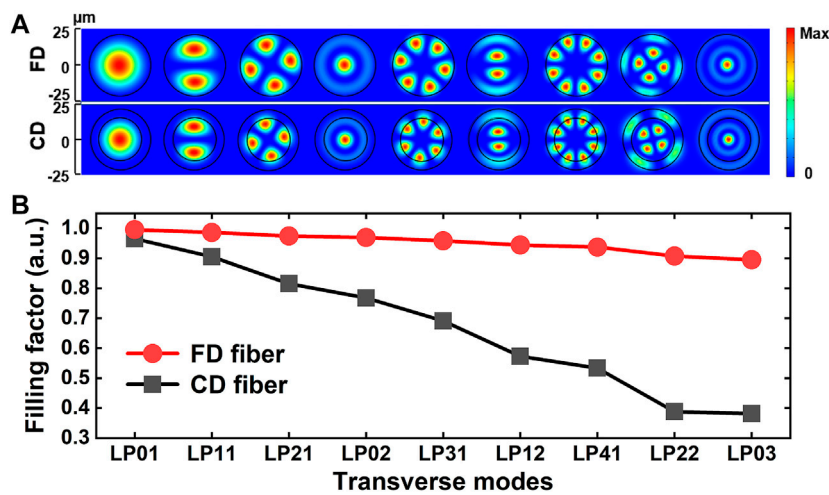


FIGURE 3 (A) Distribution of different modes in the full-doped (FD) or confined-doped (CD) fiber; (B) the signal power filling factors of different modes in the FD or CD fiber.

shown in the bottom half are relatively small (in the confined-doped fiber). This is caused by the difference in refractive index distribution within the core due to the confined-doped technique, which leads to the convergence of the beam profile to the central region of the fiber core [38]. Further, we calculate the signal filling factors (Γ_i) of those 9 different modes which are defined as:

$$\Gamma_i = \frac{\int_0^{r_1} \int_0^{2\pi} r \psi_i(r, \varphi) dr d\varphi}{\int_0^{r_2} \int_0^{2\pi} r \psi_i(r, \varphi) dr d\varphi}, \quad (2)$$

among which r_1 and r_2 represent to the radiuses of the doped region and cladding, and $\psi_i(r, \varphi)$ denotes the intensity distribution of mode i . The calculated result has been illustrated in Figure 3B. Comparing with the full-doped fiber, the confined-doped fiber shows significant decreases in signal filling factors for the high-order modes, indicating a salient performance of the confined-doped fiber on providing preferential gain for the fundamental mode.

Experiment results

In the experiment, the performance of the full-doped fiber assisted amplifier is firstly studied. Figures 4A,B demonstrate the temporal traces and the beam qualities measured at 195 W and 219 W (representing to the power level before and after the TMI threshold). As we can see, when the output power is scaled to 195 W, the temporal trace remains stable and the classical beam quality (M^2 factor) for the x/y direction is measured to be 1.60/1.59. Besides, we did a numerical

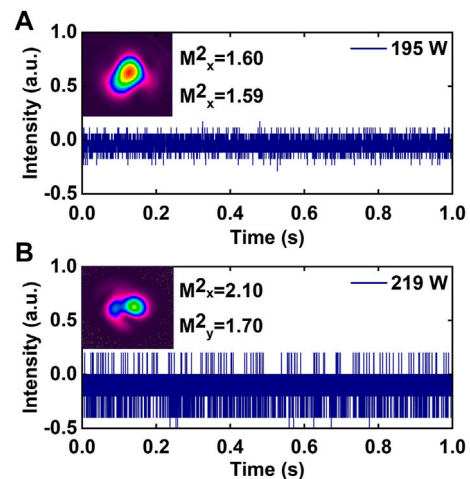


FIGURE 4 Temporal trace and the beam quality of the output laser, measured at (A) 195 W; (B) 219 W.

mode decomposition to the beam profile by using the method mentioned in Ref. [43]. The fundamental mode (FM, LP_{01}) shares 89.5% of the total power, while high-order modes (HM, mainly LP_{11}) shares 10.5%. Further improve the power to 219 W, obvious fluctuation in the temporal trace occurs, indicating the onset of TMI effect. Meanwhile, the beam quality degrades quickly and the M^2 factor is measured to be 2.10/1.70 for the x/y direction. This time, the FM shares 48.8% of the total power, while the HM (mainly LP_{11}) shares 51.2%. In addition, the beam profile of

the output laser is slightly out of Gaussian shape before the TMI threshold, and which are severely deviates from Gaussian shape after the TMI threshold in the full-doped fiber assisted amplifier. Over all, full-doped technique in such large-mode area fiber is not a suitable choice to achieve high-power single-frequency lasers with excellent beam quality.

Based on the confined-doped fiber constructed all-fiber single-frequency amplifier, we make a detail investigation on the power scaling and single-mode operating properties of the confined-doped fiber. The main characteristics of the injected seed laser as well as the amplified signal laser have been demonstrated in the following content. The spectrum and beam quality of the seed laser at the full power of the pre-amplifiers are studied firstly. As shared in Figure 5, there is no ASE observed in the spectrum and the SNR is measured over 56 dB, indicating a pure injection. Meanwhile, the beam quality is measured by a commercial beam quality analyzer with M^2 value of 1.25 and 1.28 for the x and y direction. The beam profile recorded at the focus point is shown inserted in Figure 5, which illustrates that the injected seed is operated at near-diffraction-limited beam quality.

Then, the performance of the confined-doped fiber on power scaling and single-mode operating throughout the power amplification process is investigated. Figure 6A illustrates the output power as well as the backward power versus the pump power. Through the power amplification, the output power arises linearly with the pump power and the slope efficiency is measured to be 70.1%. When the output power exceeds 256 W (pumped by 360 W), there is a significant nonlinear increase in the backward power, indicating the onset of SBS effect. In this paper, the SBS threshold is defined as the output power when the proportion of the backward power to the output power

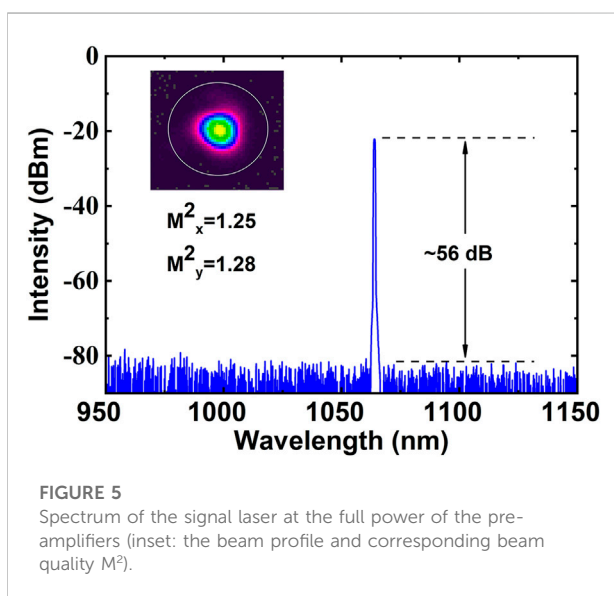


FIGURE 5
Spectrum of the signal laser at the full power of the pre-amplifiers (inset: the beam profile and corresponding beam quality M^2).

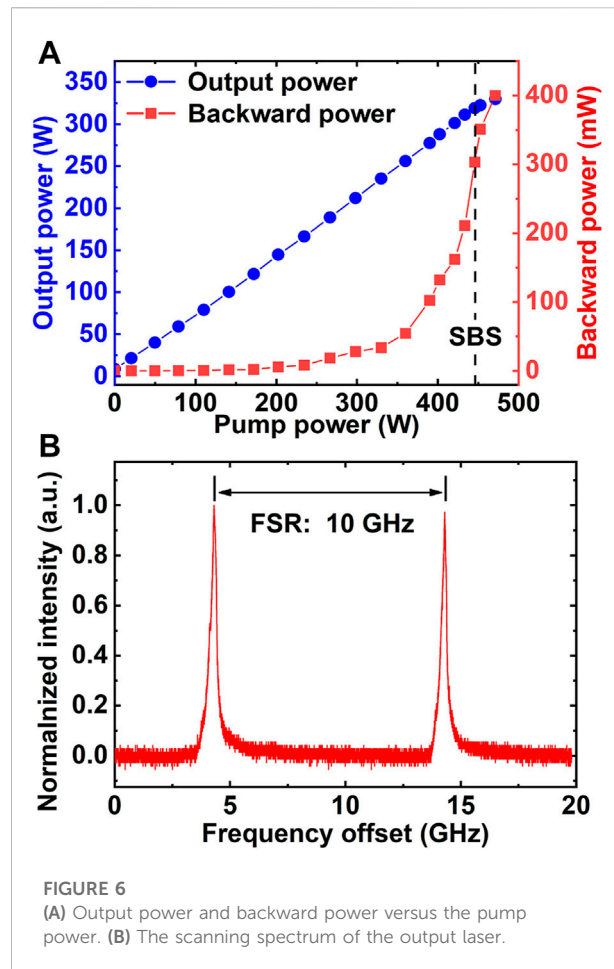


FIGURE 6
(A) Output power and backward power versus the pump power. (B) The scanning spectrum of the output laser.

reaches 0.1%. As shown in the Figure 6A, the SBS threshold of this amplifier is measured to be 322 W (pumped by 452 W). Figure 6B is the scanning spectrum of the output laser, which is measured by a Fabry-Perot interferometer (FPI) with a free spectral range (FSR) of 10 GHz. This figure illustrates that the signal laser is operating in the single-frequency state. Further, in cooperation with a Michelson interferometer composed of a 3×3 optical fiber coupler [44], the spectral linewidth of the output laser is measured to be 37.5 kHz, 29.1 kHz, and 21.3 kHz at the integral time of 5 ms, 1 ms, and 0.3 ms at the maximum output power.

The spectral information of the signal laser and backward propagating laser is shared in Figure 7. At the maximum output power, the spectrum of the output signal laser is recorded and shown in Figure 7A. As shown in this picture, the intensity of the output signal is ~ 48 dB higher than the pump laser and ~ 62 dB higher than the ASE component, i.e., the confined-doped fiber provides a great suppression of ASE effect. Meanwhile, the spectral of the backward propagating light are measured at the output power of 134 W, 256 W and 322 W, which are shared in

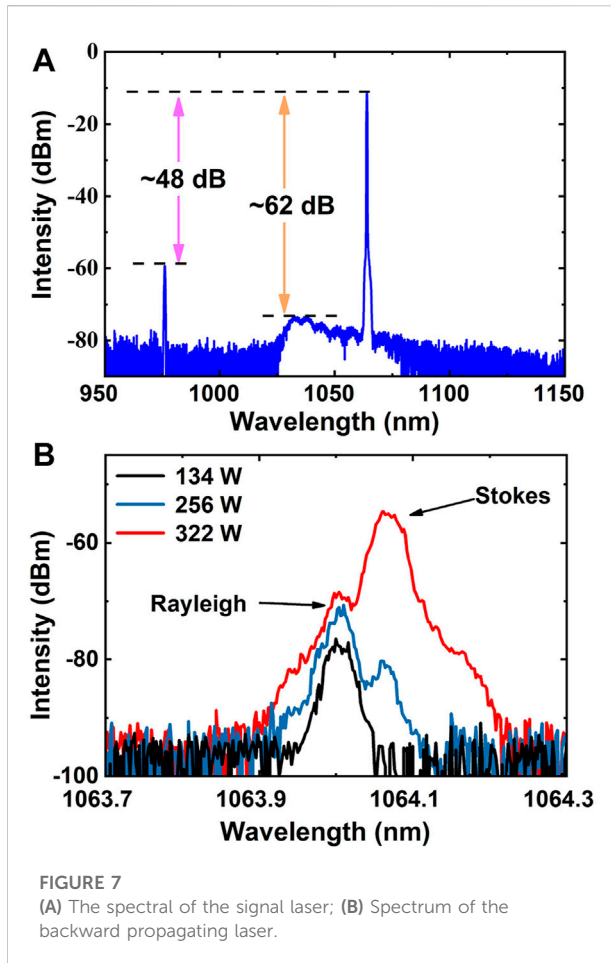
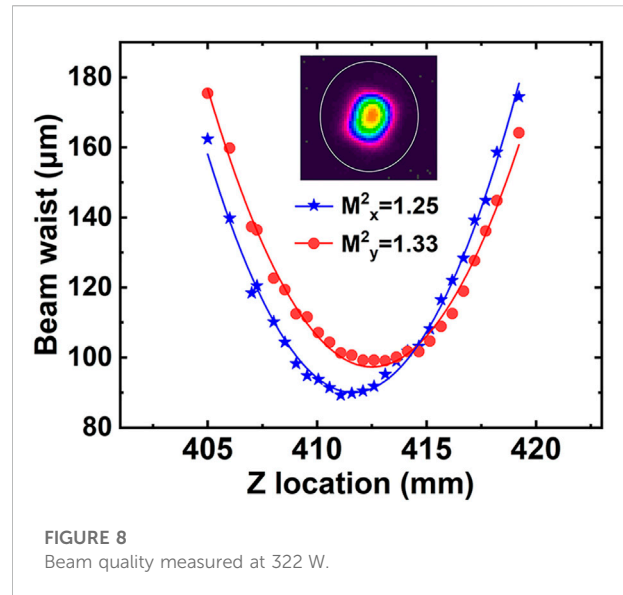


Figure 7B. As shown in the picture, two peaks could be found in the spectrum when the output power is amplified over 256 W, representing to the Rayleigh scattered light and the Stokes light induced by the SBS effect. The central wavelength of the Rayleigh scattered light is $\sim 1,064.00$ nm (the same as the signal). As for the Stokes light, an obvious frequency shift is observed in the spectrum, which is measured to be ~ 0.06 nm. Especially, after the onset of SBS effect, the intensity of the Stokes light increases quickly. And at the maximum output power, the intensity of Stokes peak is ~ 14 dB above that of the Rayleigh peak, namely, Stokes light has dominated the power composition of backwards light.

Subsequently, the beam quality of the output laser is also measured at the maximum output power, as shown in Figure 8. Due to the distortion of the beam profile, there is a slight difference in the beam waist for the x and y directions. And the focused location of x direction is at ~ 412 mm while that of the y direction is at ~ 413 mm. The inserted picture is the near-field intensity profile of the output laser (demonstrating in a near-Gaussian shape), which is recorded at the Z location of 412.6 mm. At this time, the beam quality is measured with M^2 value of 1.25 and 1.33 in the



x and y directions, respectively. Overall, the beam quality value and the near-Gaussian shape intensity profile proves that the amplifier is working at a near-diffraction-limited beam quality. Comparing with the beam quality of the injected seed (shown in Figure 5), only a slight degradation in beam quality is observed, indicating that the confined-doped fiber performs well in beam quality maintaining in single-frequency lasers with near-diffraction-limited beam quality.

Conclusion

In this paper, we investigated the power scaling and beam quality maintaining capability of the confined-doped fiber with core/cladding diameter of $42.0/250.0$ μm (the doping ratio is fabricated at $\sim 71.5\%$) in all-fiber single-frequency amplifiers. Based on this all-fiber amplifier, a 322 W single-frequency laser was achieved and further power scaling is only limited by the SBS effect. Benefit from the single-mode operation feature of the confined-doped fiber and proper coiling of the active fiber, great beam quality is obtained with M^2 value of 1.25 and 1.33 for the x and y direction. Comparing with the full-doped fiber assisted amplifier, both the TMI threshold and beam quality of the confined-doped fiber assisted amplifier have been significantly improved. This result confirms the excellent performance of the confined-doped fiber for power scaling and single-mode operating in all-fiber single-frequency fiber amplifiers. It also provides a well reference of the comprehensive suppression of the SBS and TMI effects in all-fiber single-frequency lasers.

Data availability statement

The raw data supporting the conclusions of this article will be made available by the authors, without undue reservation.

Author contributions

All authors listed have made a substantial, direct, and intellectual contribution to the study and approved it for publication.

Funding

This work was supported by the National Natural Science Foundation of China (62075242, 62005313, 62035015).

References

- Chang H, Chang Q, Xi J, Hou T, Su R, Ma P, et al. First experimental demonstration of coherent beam combining of more than 100 beams. *Photon Res* (2020) 8(12):1943–8. doi:10.1364/prj.409788
- De Varona O, Fittkau W, Booker P, Theeg T, Steinke M, Kracht D, et al. Single-frequency fiber amplifier at 15 μm with 100 W in the linearly-polarized TEM₀₀ mode for next-generation gravitational wave detectors. *Opt Express* (2017) 25(21):24880–92. Epub 2017/10/19. doi:10.1364/OE.25.024880
- Wellmann F, Steinke M, Meylahn F, Bode N, Willke B, Overmeyer L, et al. High power, single-frequency, monolithic fiber amplifier for the next generation of gravitational wave detectors. *Opt Express* (2019) 27(20):28523–33. Epub 2019/11/07. doi:10.1364/OE.27.028523
- Yang F, Ye Q, Pan Z, Chen D, Cai H, Qu R, et al. 100-Mw linear polarization single-frequency all-fiber seed laser for coherent Doppler lidar application. *Opt Commun* (2012) 285(2):149–52. doi:10.1016/j.optcom.2011.09.030
- Kumar SC, Samanta GK, Ebrahim-Zadeh M. High-power, single-frequency, continuous-wave second-harmonic-generation of ytterbium fiber laser in ppkt and mgo:spplt. *Opt Express* (2009) 17(16):13711–26. Epub 2009/08/06. doi:10.1364/oe.17.013711
- Zhang L, Yuan Y, Liu Y, Wang J, Hu J, Lu X, et al. 589 Nm laser generation by frequency doubling of a single-frequency Raman fiber laser in ppslt. *Appl Opt* (2013) 52(8):1636–40. Epub 2013/03/13. doi:10.1364/AO.52.001636
- Huang L, Lai W, Ma P, Wang J, Su R, Ma Y, et al. Tapered Yb-doped fiber enabled monolithic high-power linearly polarized single-frequency laser. *Opt Lett* (2020) 45(14):4001–4. Epub 2020/07/16. doi:10.1364/OL.393051
- Lee Y-W, Digonnet MJF, Sinha S, Urbanek KE, Byer RL, Jiang S. High-power Yb^{3+} -Doped phosphate fiber amplifier. *IEEE J Sel Top Quan Electron* (2009) 15(1):93–102. doi:10.1109/jstqe.2008.2010263
- Kobyakov A, Sauer M. Stimulated Brillouin scattering in optical fibers. *Adv Opt Photon* (2010) 2:1–59. Epub 2009/12/17. doi:10.1364/aop.2.000001
- Gray S, Liu A, Walton DT, Wang J, Li MJ, Chen X, et al. 502 watt, single transverse mode, narrow linewidth, bidirectionally pumped Yb-doped fiber amplifier. *Opt Express* (2007) 15(25):17044–50. Epub 2007/12/10. doi:10.1364/oe.15.017044
- Boggio JMC, Marconi JD, Fragnito HL. Experimental and numerical investigation of the sbs-threshold increase in an optical fiber by applying strain distributions. *J Lightwave Technol* (2005) 23(11):3808–14. doi:10.1109/jlt.2005.856226
- Kovalev VI, Harrison RG. Suppression of stimulated Brillouin scattering in high-power single-frequency fiber amplifiers. *Opt Lett* (2006) 31(2):161–3. Epub 2006/01/31. doi:10.1364/ol.31.000161
- Lou Z, Han K, Wang X, Zhang H, Xu X. Increasing the sbs threshold by applying a flexible temperature modulation technique with temperature measurement of the fiber core. *Opt Express* (2020) 28(9):13323–35. Epub 2020/05/15. doi:10.1364/OE.389333
- Dajani I, Zeringue C, Lu C, Vergien C, Henry L, Robin C. Stimulated Brillouin scattering suppression through laser gain competition scalability to high power. *Opt Lett* (2010) 35(18):3114–6. doi:10.1364/OL.35.003114

Conflict of interest

The authors declare that the research was conducted in the absence of any commercial or financial relationships that could be construed as a potential conflict of interest.

Publisher's note

All claims expressed in this article are solely those of the authors and do not necessarily represent those of their affiliated organizations, or those of the publisher, the editors and the reviewers. Any product that may be evaluated in this article, or claim that may be made by its manufacturer, is not guaranteed or endorsed by the publisher.

- Lai W, Ma P, Song J, Ren S, Liu W, Zhou P. Kilowatt-level, narrow linewidth, polarization-maintained all-fiber amplifiers based on multi-phase coded signal modulation and laser gain competition. *Results Phys* (2021) 2021:105050. doi:10.1016/j.rinp.2021.105050
- Zeringue C, Vergien C, Dajani I. Pump-limited, 203 W, single-frequency monolithic fiber amplifier based on laser gain competition. *Opt Lett* (2011) 36(5):618–20. Epub 2011/03/04. doi:10.1364/OL.36.000618
- Theeg T, Sayinc H, Neumann J, Kracht D. All-fiber counter-propagation pumped single frequency amplifier stage with 300-W output power. *IEEE Photon Technol Lett* (2012) 24(20):1864–7. doi:10.1109/lpt.2012.2217487
- Wellmann F, Steinke M, Wessels P, Bode N, Meylahn F, Willke B, et al. Performance study of a high-power single-frequency fiber amplifier architecture for gravitational wave detectors. *Appl Opt* (2020) 59(26):7945–50. Epub 2020/09/26. doi:10.1364/AO.401048
- Hejaz K, Norouzey A, Poozesh R, Heidariazar A, Roohforouz A, Rezaei Nasirabad R, et al. Controlling mode instability in a 500 W ytterbium-doped fiber laser. *Laser Phys* (2014) 24(2):025102. doi:10.1088/1054-660x/24/2/025102
- Tao R, Su R, Ma P, Wang X, Zhou P. Suppressing mode instabilities by optimizing the fiber coiling methods. *Laser Phys Lett* (2017) 14(2):025101. doi:10.1088/1612-202X/aa4fbf
- Deng H, Chen D, Zhao Q, Yang C, Zhang Y, Zhang Y, et al. An efficient low-noise single-frequency 1033 Nm Yb^{3+} -doped mopa phosphate fiber laser system. *J Opt* (2017) 19(6):065502. doi:10.1088/2040-8986/aa674f
- Naderi NA, Dajani I, Flores A. High-efficiency, kilowatt 1034 Nm all-fiber amplifier operating at 11 Pm linewidth. *Opt Lett* (2016) 41(5):1018–21. Epub 2016/03/15. doi:10.1364/OL.41.001018
- Tao R, Ma P, Wang X, Zhou P, Liu Z. Mitigating of modal instabilities in linearly-polarized fiber amplifiers by shifting pump wavelength. *J Opt* (2015) 17(4):045504. doi:10.1088/2040-8978/17/4/045504
- Jauregui C, Stihler C, Tunnermann A, Limpert J. Pump-modulation-induced beam stabilization in high-power fiber laser systems above the mode instability threshold. *Opt Express* (2018) 26(8):10691–704. Epub 2018/05/03. doi:10.1364/OE.26.010691
- Stihler C, Jauregui C, Kholaf SE, Limpert J. Intensity noise as a driver for transverse mode instability in fiber amplifiers. *Photonix* (2020) 1(1):8. doi:10.1186/s43074-020-00008-8
- Smith AV, Smith JJ. Increasing mode instability thresholds of fiber amplifiers by gain saturation. *Opt Express* (2013) 21(13):15168–82. Epub 2013/07/12. doi:10.1364/OE.21.015168
- Tao R, Ma P, Wang X, Zhou P, Liu Z. 1.3 Kw monolithic linearly polarized single-mode master oscillator power amplifier and strategies for mitigating mode instabilities. *Photon Res* (2015) 3(3):86–93. doi:10.1364/prj.3.000086
- Robin C, Dajani I, Pulford B. Modal instability-suppressing, single-frequency photonic crystal fiber amplifier with 811 W output power. *Opt Lett* (2014) 39(3):666–9. Epub 2014/02/04. doi:10.1364/OL.39.000666

29. Wu H, Li R, Xiao H, Huang L, Yang H, Leng J, et al. First demonstration of a bidirectional tandem-pumped high-brightness 8 Kw level confined-doped fiber amplifier. *J Lightwave Technol* (2022) 40(16):5673–81. doi:10.1109/jlt.2022.3183381
30. Tao R, Wang X, Zhou P. Comprehensive theoretical study of mode instability in high-power fiber lasers by employing a universal model and its implications. *IEEE J Sel Top Quan Electron* (2018) 24(3):1–19. doi:10.1109/jstqe.2018.2811909
31. Jauregui C, Stihler C, Limpert J. Transverse mode instability. *Adv Opt Photon* (2020) 12(2):429–84. doi:10.1364/aop.385184
32. Shi C, Fu S, Deng X, Sheng Q, Xu Y, Fang Q, et al. 435 W single-frequency all-fiber amplifier at 1064 Nm based on cascaded hybrid active fibers. *Opt Commun* (2022) 2022:127428. doi:10.1016/j.optcom.2021.127428
33. Matniyaz T, Bingham SP, Kalichevsky-Dong MT, Hawkins TW, Pulford B, Dong L. High-power single-frequency single-mode all-solid photonic bandgap fiber laser with khz linewidth. *Opt Lett* (2022) 47(2):377–80. Epub 2022/01/15. doi:10.1364/OL.449412
34. Lai W, Ma P, Liu W, Huang L, Li C, Ma Y, et al. 550 W single frequency fiber amplifiers emitting at 1030 Nm based on a tapered Yb-doped fiber. *Opt Express* (2020) 28(14):20908–19. Epub 2020/07/19. doi:10.1364/OE.395619
35. Hochheim S, Brockmuller E, Wessels P, Koponen J, Lowder T, Novotny S, et al. Single-frequency 336 W spliceless all-fiber amplifier based on a chirally-coupled-core fiber for the next generation of gravitational wave detectors. *J Lightwave Technol* (2022) 40(7):2136–43. doi:10.1109/jlt.2021.3133814
36. Marcianti JR, Roides RG, Shkunov VV, Rockwell DA. Near-diffraction-limited operation of step-index large-mode-area fiber lasers via gain filtering. *Opt Lett* (2010) 35(11):1828–30. Epub 2010/06/03. doi:10.1364/OL.35.001828
37. Wang B, Pang L, Liu J, Wang T, Chai T, Fan H, et al. Single mode 2.4kw part-doped ytterbium fiber fabricated by modified chemical vapor deposition technique. *Proc SPIE* 11427(2020). p. 114271X. doi:10.1117/12.2551991
38. Wu H, Li R, Xiao H, Huang L, Yang H, Pan Z, et al. High-power tandem-pumped fiber amplifier with beam quality maintenance enabled by the confined-doped fiber. *Opt Express* (2021) 29(20):31337–47. Epub 2021/10/08. doi:10.1364/OE.435829
39. Cooper MA, Gausmann S, Antonio-Lopez JE, Schülzgen A, Amezcua-Correa R, Jáuregui-Misas C, et al. Confined doping lma fibers for high power single frequency lasers. *Proc SPIE*(2022). 2022. 1198106. doi:10.1117/12.2610200
40. Zhao Q, Xu S, Zhou K, Yang C, Li C, Feng Z, et al. Broad-bandwidth near-shot-noise-limited intensity noise suppression of a single-frequency fiber laser. *Opt Lett* (2016) 41(7):1333–5. Epub 2016/05/19. doi:10.1364/OL.41.001333
41. Kouznetsov D, Moloney JV. Efficiency of pump absorption in double-clad fiber amplifiers. Ii. Broken circular symmetry. *J Opt Soc Am B* (2002) 19(6):1259–63. doi:10.1364/josab.19.001259
42. Liu A, Ueda K. The absorption characteristics of circular, offset, and rectangular double-clad fibers. *Opt Commun* (1996) 132:511–8. doi:10.1016/0030-4018(96)00368-9
43. An Y, Li J, Huang L, Li L, Leng J, Yang L, et al. Numerical mode decomposition for multimode fiber: From multi-variable optimization to deep learning. *Opt Fiber Tech* (2019) 2019:101960. doi:10.1016/j.yofte.2019.101960
44. Xu D, Yang F, Chen D, Wei F, Cai H, Fang Z, et al. Laser phase and frequency noise measurement by Michelson interferometer composed of a 3×3 optical fiber coupler. *Opt Express* (2015) 23(17):22386–93. Epub 2015/09/15. doi:10.1364/OE.23.022386